Communications Earth & Environment https://doi.org/10.1038/s43247-026-03610-z

Article in Press

Inorganic carbon fixation by deep prokaryotes as an unaccounted-for CO_2 sink in Antarctic waters

Received: 19 August 2025

Accepted: 30 April 2026

Cite this article as: Celussi, M., Manna, V., Quero, G.M. *et al.* Inorganic carbon fixation by deep prokaryotes as an unaccounted-for CO_2 sink in Antarctic waters. *Commun Earth Environ* (2026). https://doi.org/10.1038/s43247-026-03610-z

Mauro Celussi, Vincenzo Manna, Grazia Marina Quero, Elisa Banchi, Marco Basili, Giorgio Budillon, Pasquale Castagno, Andrew P. Rees & Gian Marco Luna

Inorganic carbon fixation by deep prokaryotes as an unaccounted-for CO_2 sink in Antarctic waters

Mauro Celussi[1*], Vincenzo Manna[1], Grazia Marina Quero[2], Elisa Banchi[1], Marco Basili[2], Giorgio Budillon[3], Pasquale Castagno[4], Andrew P. Rees[5], Gian Marco Luna[2]

[1] National Institute of Oceanography and Applied Geophysics - OGS, v. Piccard 54, 34151 Trieste, Italy

[2] Consiglio Nazionale delle Ricerche, Istituto per le Risorse Biologiche e le Biotecnologie Marine (CNR-IRBIM), Largo Fiera della Pesca 2, 60125 Ancona, Italy

[3] Università degli Studi di Napoli Parthenope, Centro Direzionale, Isola C4; 80143 Naples, Italy

[4] Università degli Studi di Messina, Viale Ferdinando Stagno d'Alcontres, 31, 98166 Messina, Italy

[5] Plymouth Marine Laboratory, Prospect Place, The Hoe, Plymouth, PL1 3DH, United Kingdom

* Corresponding author mcelussi@ogs.it

Abstract

The Ross Sea is one of the most productive regions of the Ocean and is a major site of deep-water formation, ultimately affecting the global thermohaline circulation. As such, it plays a pivotal role in regulating atmospheric CO_2 through the biological and the solubility carbon pumps. Despite the recognised importance of this area, the knowledge of the carbon fluxes mediated by microbes in its interior remains limited. Here we describe the outcomes of 62 incubation experiments aimed at understanding the processing of inorganic and organic carbon pools between 200 and 2000m. Results showed that in these waters DIC fixation occurs at rates between 0.03 and 3.12 nmolC L^{-1} d^{-1} and represents a relevant CO_2 sink, especially under high particulate organic carbon conditions. Both Archaea (Nitrosopumilaceae) and Bacteria (SUP05 and SAR324) were identified as putative major DIC fixers in High Salinity Shelf Water, Circumpolar Deep Water, and Antarctic Bottom Water.

Introduction

A sound knowledge of the functioning of the oceanic C cycle is essential for predicting the consequences of CO_2 increase in the atmosphere. Classically, the dark ocean, which accounts for 95% of the Earth's biosphere[1], has been considered a purely heterotrophic environment dominated by the mineralization of organic matter exported from the surface layers[2]. However, recent data suggest that the amount of CO_2 (*sensu* DIC = Dissolved Inorganic Carbon) fixed in deep ocean systems is comparable to the amount taken up by photosynthetic organisms in the illuminated part of the water column[3,4,5]. Dark DIC fixation is carried out by both chemoautotrophs and heterotrophs. Chemoautotrophs in the Ocean obtain energy from the oxidation of reduced compounds such as ammonia[6], nitrite[7], sulphur species[8], etc. and incorporate DIC for biomass build-up. Heterotrophs incorporate inorganic carbon through several carboxylation reactions, that are integral to their central and peripheral metabolic pathways[9], addressed

at the synthesis of fatty acids, amino acids and nucleotides as an extra source of C in oligotrophic conditions[10] or to cope with pulsed inputs of organic material[11].

The Southern Ocean represents about 10% of the world's oceans[12], yet it plays a crucial role in ventilating the global ocean and absorbing approximately 10% of anthropogenic CO_2 emissions[13,14]. Despite being a high nutrient-low chlorophyll system due to the limiting concentrations of critical micronutrients, and in particular iron[15,16], its marginal seas are primary production hotspots[17]. Notably, the Ross Sea is one of the most productive regions in the Southern Ocean, contributing to one-third of its annual productivity and over 25% of its total CO_2 uptake[18,19]. About half of the carbon fixed by surface-dwelling primary producers is exported as particulate organic matter (POM) to the mesopelagic zone, potentially accounting for up to 40% of global POM export[2,20]. During winter, the lack of light severely limits photosynthesis and subsequent carbon export[21]; therefore, planktonic microbial communities are sustained by the Dissolved Organic Carbon (DOC) accumulated in summer and by dark DIC fixation, which corresponds to ca. 10% of total prokaryotic production[22].

As a critical site of deep-water formation[23], the Ross Sea plays a pivotal role in the sequestration of CO_2 to the deep ocean. Dense shelf waters, originated mainly during winter, sink and contribute to the formation of Antarctic Bottom Water (AABW), the most voluminous water mass in the deep ocean (30-40%)[24], which supports the lower cell (*i.e.* the deep thermohaline-driven limb of the ocean conveyor belt) of the global overturning circulation[25]. In detail, in the western sector of the Ross Sea (Fig. 1), the most important dense shelf water is High Salinity Shelf Water (HSSW), formed mainly in Terra Nova Bay, characterised by salinities > 34.75, potential temperature (Θ) below -1.58°C and rich in oxygen (ca. 280-295 µmol L^{-1}). HSSW spreads both southward toward the Ross Ice Shelf cavity and northward along the Drygalski basin toward the shelf break off Cape Adare where it mixes with Circumpolar Deep Water (CDW). CDW is the most voluminous water mass of the Southern Ocean; it flows westward around the continent and, in the Ross Sea area, it forms a thick layer (> 1013 m) everywhere along the slope. It is an old, warm (Θ > 0.6°C), oxygen-poor (ca. 190-200 µmol L^{-1}) and nutrient-rich water mass (NO_3^-: ~ 30-33 µmol L^{-1}; PO_4^{3-}: ~ 2-2.5 µmol L^{-1}). The mixing of CDW and HSSW generates AABW, a deep water mass with a neutral density > 28.27 kg m^{-3}, which holds intermediate biogeochemical features[26,27,28].

Despite the cornerstone role that the Southern Ocean plays in the global carbon budget, very little information is available on the biodiversity and metabolism of the deep microbiome in its marginal seas and in the Ross Sea in particular.

In this work, we discuss 62 incubation experiments performed during two summertime cruises in the western Ross Sea which aimed at understanding the processing of inorganic and organic C pools in HSSW, CDW and AABW between ca. 200 and 2000 m depths (Fig. 1; Supplementary Table 1). We investigated the DIC uptake (by chemosynthesis or anaplerosis) and production (by respiration), as well as the utilization of dissolved organic carbon (by heterotrophic production) and its release (by excretion or viral lysis). Our overarching hypothesis was that in CDW, the oldest, oxygen-poor water mass, chemoautotrophy could help supply microbial communities with freshly-produced organic carbon, whereas in the youngest, POM-rich HSSW heterotrophic processes would predominate. Results showed that in these waters DIC fixation occurs at rates comparable to those measured in most oceanic regions and could account for 5% of the currently estimated yearly CO_2 sink in the Ross Sea. Higher DIC fixation occurred in high POM conditions, thus suggesting a priming effect of organic particles. Autotrophic/mixotrophic prokaryotes were abundant and evenly distributed in the three water masses,

suggesting that chemolithotrophic pathways do not prevail in one specific water mass, but are ubiquitous to all three.

Results and Discussion

Environmentally driven metabolism of deep-sea microbes in the Ross Sea

Our survey was conducted during two summer cruises and, in both expeditions, samples were collected in High Salinity Shelf Water, Circumpolar Deep Water and Antarctic Bottom Water. The biogeochemical setting did not display substantial interannual variability, with few exceptions regarding POC, PN, NO_3^- and NH_4^+ whose concentrations were slightly lower during the first cruise in CDW and AABW (Supplementary Figure 1). Interannual variations in the water masses' chemistry have already been described and attributed mainly to differences in yearly HSSW formation, and consequent differential mixing with CDW at the shelf break[27]. Overall, CDW was enriched in NO_3^- (33.43 ± 0.76 µmol L^{-1}) and PO_4^{3-} (2.02 ± 0.12 µmol L^{-1}) if compared to HSSW (31.35 ± 0.56 and 1.97 ± 0.07 µmol L^{-1}, respectively) (Supplementary Figure 2). NH_4^+ concentration did not vary among water masses (overall mean ± SD = 0.17 ± 0.08 µmol L^{-1}), whereas the highest NO_2^- load was observed in AABW (0.04 ± 0.01 µmol L^{-1}). Important differences among water masses were observed in the organic matter pool. In fact, samples collected in HSSW were richer in POC (0.97 ± 0.50 µmol L^{-1} in HSSW vs. 0.64 ± 0.34 µmol L^{-1} in CDW), poorer in DOC (48.37 ± 6.04 µmol L^{-1} in HSSW vs. 58.56 ± 12.62 µmol L^{-1} in CDW) and their C/N ratio indicated a more bioavailable pool of dissolved organic matter[29] (15.16 ± 3.12 in HSSW vs 24.73 ± 11.24 in CDW (Fig. 2). In fact, the stoichiometry of the organic matter pool, and in particular the ratio between C and N is indicative of the bioavailability or the age of substrates, since proteinaceous, N-rich molecules are utilised more quickly by degrading microbes, resulting in an enrichment of C-rich compounds, both in the particulate[30] and the dissolved[29] pools. Altogether, these results reflect the high biological productivity of HSSW formation areas[19], where pronounced organic matter synthesis by phytoplankton reflects in high export of particulate organic matter[20], and sinking particles are subjected to a continuous release of dissolved compounds by the hydrolytic activity of particle-attached microbes[30].

In such an environmental scenario, microbial activities were generally enhanced in HSSW if compared to CDW, being influenced by the organic matter pool and features (Fig. 3 and Supplementary Figure 3). In particular, both Heterotrophic C Production (HCP) and respiration rates were highest in HSSW (HCP: 33.25 ± 16.29 nmol C L^{-1} d^{-1} in HSSW vs. 1.86 ± 1.34 nmol C L^{-1} d^{-1} in CDW; Respiration with 0.68 conversion factor: 3.70 ± 1.88 nmol C L^{-1} d^{-1} in HSSW vs. 16.71 ± 9.33 nmol C L^{-1} d^{-1} in CDW) and correlated positively with POC and negatively with dissolved C/N (Spearman's ρ: POC vs HCP = 0.54, N = 62, $p < 0.001$; POC vs Respiration = 0.53, N = 61, $p < 0.001$; C/N vs HCP = -0.40, N = 36 $p = 0.017$; C/N vs Respiration = -0.37, N = 36, $p = 0.027$). Results about these metabolic features are subjected to the choice of conversion factors (CF). While the Leucine-to-Carbon CF in the deep-sea literature can vary by approximately two-fold[31], CFs for computing respiration rates with the ETS method can span two orders of magnitude[32]. In this study for HCP we adopted the commonly used 1.55 kg C mol^{-1} leucine in order to be able to compare our results with most literature reports. For respiration two different CFs were used (see Methods), being the ones that resulted in the most likely prokaryotic growth efficiency according to literature findings[33] (Supplementary Figure 4). Bearing these caveats in mind, in this study our purpose was to establish a comparison among the water masses, therefore we show both alternatives for rates calculations (Fig. 3, Supplementary Figure 4).

DIC uptake rates ranged between 0.03 ± 0.00 and 3.12 ± 0.49 nmol C L^{-1} d^{-1} (Fig. 3) and highlighted values comparable to those assessed elsewhere in the world's oceans (Table 1) despite the lower temperatures. Notably, we were not able to detect a measurable release of newly produced organic matter (excreted radiolabelled DOC), differently from what has been observed in culture[34] and in the deep Mediterranean Sea[3,35]. The very few reported values of dark DIC fixation for Antarctic waters[22,36,37] are consistent with the data presented here (Table 1). Higher rates have been observed in association with the McMurdo Ice Shelf cavity (6.0 ± 1.0 nmol C L^{-1} d^{-1})[36], which is inhabited by abundant and active chemoautotrophic organisms[38]. On average (±SD), the ratio between DIC uptake and HCP was 0.21 ± 0.16 in AABW, 0.28 ± 0.22 in CDW, and 0.38 ± 0.20 in HSSW, in line with values computed in several water masses of the western basin of the North Atlantic[39].

Interestingly, as observed for HCP and respiration, DIC uptake in HSSW was higher (three-fold on a median basis) than rates measured in the other water masses (Fig. 3).

Particles in the ocean are hotspots of microbial activities due to their high content of inorganic nutrients and organic substrates (e.g. Azam and Long, 2001[30]); therefore, it is not surprising that higher heterotrophic activities are measured in systems with high POC content[37]. However, high rates of DIC fixation in the deep ocean have been attributed to two contrasting mechanisms. In the first, the highest inorganic carbon fixation rates are observed as a direct upregulation in response to the scarcity of the DOM pool[3,40]. The second mechanism sees a priming effect by specific organic compounds which trigger this metabolic trait and the upregulation of assimilatory carboxylases involved in amino acids, nucleic acids precursors, and fatty acids biosynthetic pathways[11,37,41]. Our data suggest a third mechanism, where DIC fixation is associated with the POC load or export (Spearman's $\rho = 0.51$, $N = 61$, $p < 0.001$). So far, pronounced anaplerotic reactions in the deep sea have been considered less important than autotrophy due to the limited availability of organic carbon[5]. However, the exceptional particulate matter concentration resulting from the export of high surface water productivity typical of the Ross Sea[19], might promote DIC uptake, especially in HSSW, possibly through heterotrophic/mixotrophic pathways[40], as observed with labile organic compounds in Atlantic mesopelagic waters[11]. Likewise, a higher bioavailability of the dissolved organic matter pool in HSSW (as inferred by the C/N ratio) might be responsible for enhanced DIC utilization in this water mass (Spearman's $\rho = -0.52$, $N = 35$, $p = 0.001$). It was also interesting to observe that the prokaryotic growth efficiency computed for samples collected in the different water masses did not diverge significantly (Fig. 3). In the last couple of decades emerging evidence has indicated that, notwithstanding steep environmental gradients (e.g., vertical gradients in the water column[33]), metabolic rates of individual cells are likely to display only small variations. Indeed, our dataset corroborates these findings (Supplementary Figure 5), showing similar per cell activities in the three water masses despite significant differences in prokaryotic abundance (Fig. 3, Supplementary Figure 2, Supplementary Figure 3). Similar to our finding, in the North Atlantic Ocean it has been reported that higher prokaryotic abundances were characteristic of newly formed, particle-rich water masses[39]; therefore, we speculate that in the Ross Sea high-quality organic matter sustains a more abundant prokaryotic population in HSSW, whereas recalcitrant resources, coupled with higher relative abundances of predators[42], would be responsible for lower cell numbers in CDW. This picture would, ultimately, be responsible for the differences observed in metabolic rates between HSSW and CDW. Antarctic Bottom Water, being generated by the mixing of the aforementioned water masses, displayed intermediate biogeochemical and microbiological features (Fig. 2, Fig. 3, Supplementary Figure 1, Supplementary Figure 2, Supplementary Figure 3).

Taken together, our dark DIC fixation data account for 1 ‰ of surface photosynthetic primary production data during summer (e.g. 4-8 µmol C L^{-1} d^{-1})[43]. However, not being limited by light availability, DIC fixation occurs below 200 m all year round. Therefore, when considering the volume of AABW (2,470 km^3), HSSW (71,580 km^3) and CDW (173,140 km^3)[26] and the mean DIC fixation rates per water mass (0.58, 1.30 and 0.41 nmol C L^{-1} d^{-1}, respectively), we could assess that the dark portion of the Ross Sea is responsible for a DIC sequestration rate of ca. 2 Gg C d^{-1} (0.7 Tg C yr^{-1}) (Supplementary Table 2). This rate is equivalent to ca. 5% of the estimated CO_2 sink in the Ross Sea (13 Tg C yr^{-1})[18], thus representing a non-negligible, previously unaccounted carbon sink.

Putatively autotrophic microbes in the Ross Sea deep water masses

Given the high contribution of DIC fixation to total carbon utilization by prokaryotes in the deep Ross Sea, and aiming to identify the major players of such processes, we investigated the biodiversity of deep-sea microbes using a metabarcoding approach targeting the generic prokaryotic barcode V4-V5[44], and specific regions for Bacteria[45] and Archaea[46]. Although the knowledge of the deep-sea microbiome is far from being fully dissected, there is some information on the most abundant microorganisms living in it and, to a minor extent, on their biogeochemical relevance. For this reason, we have specifically searched for Archaea and Bacteria known for their chemoautotrophic potential. Archaea of the Nitrosopumilaceae family, in particular, are thought to contribute to a large fraction of DIC fixation in the deep ocean[5,47]. Likewise, Bacteria belonging to the phylum Nitrospinae, the SAR324, SUP05 and Arctic97B-4 groups, among others, have been regarded as important chemoautotrophs in oceanic depths[7,48,49].

An initial β-diversity analysis of the bacterial assemblages showed that the different water masses harboured specific communities and that the AABW, formed by the mixing of CDW and HSSW, retained signatures of both parental water masses (Fig. 4). This phenomenon is well documented both in polar seas[50,51,52] and at lower latitudes[35,53]. As water masses are characterized by specific physical and biogeochemical features, they exert bottom-up pressures on the selection of certain taxa[54]; in addition, since the peculiar biogeochemical fingerprint of a water mass is likely to be preserved during advection and convection processes, microbial communities are transported over long distances with minor perturbations[51,55,56]. In our dataset, Archaea represented a strikingly constant presence within the communities of all water masses at the domain level (25.9 ± 7.0% relative abundance, Supplementary Figure 6).

Nevertheless, the different water masses harboured distinct relative abundance of specific ASVs belonging to the Nitrosopumilaceae family that collectively comprised roughly half of the whole archaeal community (on average 53.9 ± 6.4, Supplementary Figure 7). Such a consistent representation of archaeal nitrifiers in our samples suggests that different water masses have a similar potential for DIC fixation associated to ammonia oxidation, although we cannot exclude that some taxa (ASVs) might be more efficient than others in autotrophic processes[34]. Moreover, several studies have pointed out that ammonia oxidation by Archaea cannot explain the high DIC fixation rates in the ocean's interior alone[39,57]. However, it has been reported that underneath the Ross Ice Shelf, archaeal ammonia oxidisers are among the most active DIC fixers, as revealed by metatranscriptomic analyses[38]. We further focused on the composition of chemoautotrophic bacteria involved in the oxidation of nitrite and reduced sulphur species (Fig. 5). Among these, the most abundant taxa were the SUP05 and the SAR324 clusters. Members of the clade SUP05 can live autotrophically by oxidising hydrogen and reduced sulphur species (elemental sulphur, sulphide, thiosulfate) and fixing inorganic carbon[8]. This cluster (Thioglobaceae family) is widely distributed in deep water masses[48,56,58], and is often found in oxygen-depleted zones, in hydrothermal vent-influenced areas[8] and in low-light, organic carbon-poor conditions[59]. In our study, this cluster represented a relevant proportion of the bacterial communities, showing higher relative abundance (Fig. 5; Supplementary Table 3) in CDW (11.38 ± 2.92%) than in HSSW (6.24 ± 2.85%). Bacteria closely related to the SUP05 cluster (UBA868) have recently been reported as the most active microbes transcribing RuBisCO and dominating the transcription of genes indicative of sulphur oxidation[60]. Oxygen concentration in the water column throughout the Ross Sea is unlikely to promote the formation of H_2S; therefore, the SUP05 bacteria must obtain the energy for

autotrophic processes from thiosulfate, S_0 or hydrogen. Likewise, SAR324 is a key taxon in the dark ocean microbiome worldwide, showing high abundance, a notable metabolic versatility, and the gene repertoire for inorganic carbon fixation[61]. Notwithstanding the lack of cultured representatives, DNA-based studies indicate that this cluster can obtain energy from the oxidation of thiosulfate[48,61] or from the oxidation of sulphite generated by taurine degradation in oxygenated waters[62], being one of the most transcriptionally active taxa in the deep-sea microbiomes[63]. In our dataset, the relative abundance of this taxon was higher in CDW than in HSSW, being on average (± SD) 6.05 ± 1.75% and 3.79 ± 1.46%, respectively (Fig. 5; Supplementary Table 3).

Even when considering all the putative chemolithotrophic taxa, we observed that the newly-formed HSSW harboured a slightly minor (relative) abundance of bacteria able to fix DIC autotrophically (14.97 ± 3.23% in HSSW vs 22.95± 3.84% in CDW).

Altogether our data indicate pronounced DIC fixation rates in deep water masses of the Ross Sea and highlight several microbial taxa as potentially responsible for such processes. Whether this fixation is imputable primarily to autotrophic or to anaplerotic processes is still to be determined, even though under organic matter-limited conditions chemosynthetic microbes were shown to play a pivotal role[5]. Further studies involving the genetic repertoire of deep microbiomes are needed to shed more light on such processes.

Methods

Sampling strategy and environmental setting

The sampling stations (Fig. 1) were selected based on previous investigations where the target water masses had been identified[23,50,64]. The sampling was performed during the XXIX and the XXXI Italian expeditions in Antarctica onboard the R/V Italica in early 2014 and 2016. Full-depth hydrographic casts and water sampling were carried out using a SBE 9/11 PLUS CTD, with dual temperature and salinity sensors mounted on a SBE 32 carousel sampler equipped with twenty-four 12-L Niskin bottles. Sampling depths were chosen according to the physical structure of the water column (salinity and potential temperature data). Details on sampling stations are reported in Supplementary Table 1; water masses were identified according to the physical features described in Budillon et al. (2003)[23]. At each selected depth, seawater was collected for the following analytical determinations: inorganic macronutrients, dissolved and particulate organic carbon and nitrogen, prokaryotic abundance, heterotrophic carbon production (HCP), planktonic respiration (ETS), dissolved inorganic C (DIC) uptake and prokaryotic diversity.

Dissolved inorganic nutrients (PO_4^{3-}, NH_4^+, NO_2^- and NO_3^-), Dissolved Organic C (DOC) and particulate organic matter (C = POC; N = PN) concentrations were determined by standard procedures as described in Quero et al. (2020)[52]. Total dissolved nitrogen was estimated as NO_3^- after wet persulfate oxidation, according to Hansen and Koroleff (1999)[65] and the organic fraction was calculated as the difference between the total and the inorganic dissolved N concentration.

Microbial abundance, activity and diversity

Total prokaryotic abundance was measured by epifluorescence microscopy in 2014 and by flow cytometry in 2016, as described by Ingrosso et al. (2022) [28] and Manna et al. (2020)[37], respectively. In the first case, samples were preserved using a 0.2 µm filtered formaldehyde solution (2% final concentration, f.c.; Fluka), then stained with a 4',6-diamidino-2-phenylindole (DAPI) solution at 1 µg mL^{-1} f.c., in the dark for 15 min. Cells were subsequently collected on 0.22 µm black polycarbonate filters (Nucleopore) and enumerated with an Olympus BX 60 F5 microscope using a UV filter set (BP 330–385 nm, BA 420 nm) at a final magnification of 1,000 ×. Three analytical replicates (3-8 mL each) were processed for each sample; for every replicate, a minimum of 200 cells were counted in at least 20 randomly selected fields. For flow cytometry analyses, 1.7 mL seawater aliquots were fixed with glutaraldehyde (0.5% f.c., Grade I for EM analyses, Sigma Aldrich). Samples were kept at 4 °C for approximately 15 min and then stored at −80 °C until analysis. Before enumeration, samples were thawed at room temperature and diluted 1:10 with 0.2 µm-filtered 1× Tris-EDTA buffer (Sigma Aldrich). They were then stained with SYBR Green I nucleic acid dye (1× f.c., Life Technologies) for 10 min in the dark at room temperature. Analyses were performed using a FACSCanto II flow cytometer (Becton Dickinson) equipped with an air-cooled 488 nm laser and standard filter configuration. Samples were run for 2 minutes at a flow rate of approximately 60 µL min^{-1}, with green fluorescence used as a trigger. Data acquisition and processing were carried out with the FACSDiva software (Becton Dickinson). The flow rate was calibrated daily, by running distilled water and determining its mass before and after analysis (at least 5 replicates). Abundances were calculated based on the recorded counts and the corresponding flow rates. Heterotrophic carbon production (HCP) was determined from the incorporation of ^{3}H-leucine[66]. Triplicate 1.7 mL aliquots and one killed control (amended with 90 µL of 100% trichloracetic acid) were spiked with 20 nM radiotracer[67,68] (50.2 Ci $mmol^{-1}$; Perkin Elmer) and incubated in the dark for 6 h at *in situ* temperature. The extraction of ^{3}H-labelled proteins was performed using the microcentrifugation protocol[69]. Radioactivity was measured with a TRI-CARB 2900 TR Liquid Scintillation Analyzer following the addition of 1 mL of scintillation cocktail (Ultima Gold™ MV; Packard). Carbon production was calculated using a conversion factor of 1.55 kgC mol^{-1} Leu incorporated, assuming no internal isotope dilution[70].

Planktonic respiration was estimated by the Electron Transport System activity method, following Packard and Williams (1981)[71] as detailed by Reinthaler et al. (2006)[72] with slight modifications. Briefly, 16 L of seawater, prefiltered through 200 µm mesh were further filtered onto precombusted GF/F filters., which were then stored at -80°C until analysis. In the laboratory, filters were transferred to polypropylene tubes containing 4 mL of phosphate buffer. Samples were kept on ice and subjected to ultrasonication (Ultrasonic Processor XL, Misonix) for 15 sec, followed by manual homogenization using a glass Potter for 2 min. The homogenate was centrifuged at 1810 x g for 10 min at 4°C. Subsequently 1 mL of the supernatant was incubated at 15°C with 3 mL of substrate solution (NADH, NADPH and sodium succinate) and 1 mL of 2-(4-iodophenyl)-3-(4-nitrophenyl)-5-phenyltetrazolium chloride (INT). Two aliquots (1 mL each) of supernatant combined with substrate solution were used as analytical replicates. After 20 min, the reaction was terminated by adding 1 mL of a formalin - sodium formate mixture. All solutions were freshly prepared. The absorbance was measured at 490 nm using a Varian Cary 100 SCAN spectrophotometer. Duplicate GF/F filters rinsed with sterile MilliQ water were used as controls. ETS activity was measured as follows:

$$\text{ETS } (\mu L\ O_2\ L^{-1}\ h^{-1}) = (60 \times S \times H \times OD_{corr}) / (1.42 \times f \times V \times t)$$

where 60 converts minutes to hours, *S* is the volume of the quenched reaction mixture (in mL), *H* is the volume of the homogenate (in mL), OD_{corr} is the absorbance of the sample corrected with the absorbance of blanks, 1.42 converts INT-formazan formed to oxygen units, *f* is the volume of the homogenate used in the reaction, *V* is the volume of the seawater sample, *t* is the reaction time. ETS activity was corrected to *in situ* temperature using the equation:

$$ETS_{INSITU}\ (\mu L\ O_2\ L^{-1}\ h^{-1}) = ETS \times e^{[-K1/R \times (1/T1 - 1/T2)]}$$

where K1 is the activation energy (15.8 Kcal mol^{-1}), R is the gas constant, T1 and T2 are the temperatures (in °K) *in situ* and in the assay respectively. Two Respiration/ETS conversion factors were compared to compute respiration rates, calculated from ETS_{INSITU} assuming a respiratory quotient = 1. The conversion factors were 0.68[73] and 5.3[72]. These calculations led to prokaryotic growth efficiency [PGE = HCP/(HCP+Respiration)] values equal to 18 ± 16 and 4 ± 8 % (average ± SD), respectively.

Rates of Dissolved Inorganic Carbon (DIC) fixation were quantified by the incorporation of $NaH^{14}CO_3$ as described in Celussi et al. (2017)[3]. Duplicate seawater subsamples and one control (40 mL) were collected from Niskin bottles into 50 mL sterile Falcon tubes and amended with 100 µL of a $NaH^{14}CO_3$ solution (46.8 mCi $mmol^{-1}$; DHI) yielding a final activity of 0.25 µCi mL^{-1}. The control was fixed with dolomite-buffered formalin (2% f.c.). Samples were incubated in the dark for 96 h at *in situ* temperature and subsequently fixed with 2% dolomite-buffered formalin. The entire volume of each replicate was filtered through 0.2 µm polycarbonate membranes (Whatman), and 10 mL of the filtrate was collected and immediately frozen at -20°C. Filters were rinsed twice with 10 mL of an autoclaved NaCl solution (3.8% w/v), acidified with HCl fumes in scintillation vials for 12-16 h, and stored at -20°C. In the laboratory, scintillation vials were filled with 5 mL of scintillation cocktail (Filter-Count™, Perkin Elmer), and radioactivity was measured by a TRI-CARB 2900 TR Liquid Scintillation Analyzer. Filtrates from each replicate and control were thawed, and 5 mL aliquots were acidified with 200 µL of HCl 0.5N for 12 to 16 h to remove inorganic carbon (pH < 2). Subsequently, 10 mL of scintillation cocktail (Ultima Gold™ XR, Perkin Elmer) was added prior to activity measurement. The filtration and the acidification steps were completed within 24 h of formalin fixation.

DIC fixation was determined according to the following equation[74]:

$$\text{DIC fixation} = (DIC \times DPM_{sample\text{-}control} \times 1.05 \times 12)/(DPM_{added} \times T)$$

where DIC is the concentration of dissolved inorganic carbon in samples (range = 2.29 - 2.30 mmol L^{-1}) determined by Ingrosso et al. (2022)[28], 1.05 is the correction factor for slower assimilation of ^{14}C than ^{12}C, 12 is the molecular weight of C, $DPM_{sample\text{-}control}$ are DPM measured in every replicate corrected for the ones in the control, DPM_{added} is the radioactivity (certified by the provider) of the $NaH^{14}CO_3$ solution added in each tube, T is incubation time. The activity in the filtrate was not measurable in any sample; therefore, we report the particulate DIC fixation rates only (> 0.2 µm).

For prokaryotic community analysis, seawater samples (5.5 L) were filtered onto 0.22 µm pore size cellulose nitrate membrane filters (Sartorius) and stored at -20°C until processing. DNA was extracted from each filter using the PowerWater™ DNA Isolation kit (QIAGEN), according to the manufacturer's instructions with a few extra steps to increase the DNA yield and quality[35]. The DNA concentration was

measured using a Qubit Fluorometer (Thermo-Fisher), and the DNA was stored at -80°C until sequencing.

For the DNA metabarcoding analysis, a combination of three barcodes was used. In all samples (45, Supplementary Table 1), the V3-V4 region of the 16S rRNA gene was amplified with the 341F and 785R universal bacterial primers[45]. Then, in order to deepen the taxonomic coverage of some marine groups and to estimate the proportion of Bacteria and Archaea[44,75], on a selected sample subset (17, Supplementary Table 1), the V4-V5 region of 16S rRNA gene was amplified using 515-Y and 926R primers[44] and, to increase the Archaea taxonomic resolution, the same region was also amplified with 517F (five oligos in the same proportion) and 958R primers[46]. Libraries were prepared following the 16S Metagenomic Sequencing Library Preparation Illumina protocol and run on an Illumina MiSeq System for a read length of 2 × 250 bp at the COGENTECH facility (Consortium for Genomic Technologies, Milan, Italy) and BMR Genomics S.r.l., Padua, Italy (www.bmr-genomics.it).

For each barcode, primers and adapter sequences were removed from raw reads with Cutadapt v. 4.5[76]. Paired-end reads were then imported and analysed in RStudio v. 4.4.0[77] using the DADA2 package v. 1.32[78]. Quality check and trimming of the reads were performed following the package instructions. Paired-end reads were subsequently grouped in amplicon sequence variants (ASVs); chimeric sequences were identified and removed from the dataset. Finally, taxonomy was assigned using a native implementation of the naive Bayesian classifier method against the SILVA database v138.1[79]. ASVs belonging to Eukarya, mitochondria, chloroplasts, and with frequency < 2 (singletons) were removed. All sequences have been submitted to the SRA Sequence Read Archive at NCBI (BioProject Accession no. PRJNA1184697, PRJNA1184714, PRJNA1196803).

Estimates of DIC fixation rates in the Ross Sea

In order to calculate the regional dark DIC fixation rates we utilised the water masses volumetric data reported by Orsi and Wiederwohl (2009)[26] for the Ross Sea: Antarctic Bottom Water = 2,470 km^3; High Salinity Shelf Water = 71,580 km^3; Circumpolar Deep Water (+ its modified counterpart MCDW) = 173,140 km^3. These three volumes were multiplied by the average DIC fixation rate computed for each water mass: Antarctic Bottom Water = 0.58 nmol C L^{-1} d^{-1}; High Salinity Shelf Water = 1.29 nmol C L^{-1} d^{-1}; Circumpolar Deep Water = 0.41 nmol C L^{-1} d^{-1} (Supplementary Table 1).

Statistical analyses

The Shapiro-Wilk test was used to assess the normality of datasets. Significant differences in the datasets characterizing the different water masses were assessed through the Kruskal-Wallis ANOVA, followed by a post hoc 'Multiple comparisons of mean ranks for all groups' (Dunn's) test, Bonferroni corrected (Statistica v.7, StatSoft).

Non-metric multidimensional scaling (nMDS) was performed on the 16S rRNA bacterial gene dataset using a Jaccard dissimilarity matrix and average linkage approach and plotted with the *ggplot2* package (v. 3.5.1)[80] in RStudio v. 4.4.0[77]. Water mass-based partitioning of 16S data was tested with PERMANOVA, using the same dissimilarity distance built for the nMDS ordination and computed through the function *adonis2* of the *vegan* package (v. 2.7-1)[81].

Data availability

All the physical, chemical and microbiological data are available in Supplementary Table 1 and at https://doi.org/10.13120/9vk3-0t31. All DNA sequences have been submitted to the SRA Sequence Read Archive at NCBI (BioProject Accession no. PRJNA1184697, PRJNA1184714, PRJNA1196803).

References

01. Whitman WB, Coleman DC, Wiebe WJ (1998) Prokaryotes: the unseen majority. Proceeding of the National Academy of Science of the USA 95: 6578-6583.

02. Ducklow HW, Steinberg DK, Buessler KO (2001) Upper Ocean carbon export and the biological pump. Oceanography 14: 50-58. https://doi.org/10.5670/oceanog.2001.06

03. Celussi M, Malfatti F, Ziveri P, Giani M, Del Negro P (2017) Uptake-release dynamics of the inorganic and organic carbon pool mediated by planktonic prokaryotes in the deep Mediterranean Sea. Environmental Microbiology 19: 1163-1175. https://doi.org/10.1111/1462-2920.13641

04. Baltar F, Herndl GJ (2019) Ideas and perspectives: is dark carbon fixation relevant for oceanic primary production estimates? Biogeosciences 16: 3793-3799. https://doi.org/10.5194/bg-16-3793-2019

05. Herndl GJ, Bayer B, Baltar F, Reinthaler T (2023) Prokaryotic life in the deep Ocean's water column. Annual Review of Marine Science 15:461-483. https://doi.org/10.1146/annurev-marine-032122-115655

06. Ingalls AE, Shah SR, Hansman RL, Aluwihare LI, Santos GM, Druffel ERM, Pearson A (2006) Quantifying archaeal community autotrophy in the mesopelagic ocean using natural radiocarbon. Proceedings of the National Academy of Science of the USA 103: 6442-6447. https://doi.org/10.1073/pnas.0510157103

07. Pachiadaki MG, Sintes E, Bergauer K, Brown JM, Record NR, Swan BK, Mathyer ME, Hallam SJ, Lopez-Garcia P, Takaki Y, Nunoura T, Woyke T, Herndl GJ, Stepanauskas R (2017) Major role of nitrite-oxidizing bacteria in dark ocean carbon fixation. Science 358: 1046-1051. https://doi.org/10.1126/science.aan8260

08. Morris RM, Spietz RL (2022) The physiology and biogeochemistry of SUP05. Annual Reviews of Marine Science 14: 261–275. https://doi.org/10.1146/annurev-marine-010419-010814

09. Erb TJ (2011) Carboxylases in Natural and Synthetic Microbial Pathways. Applied and Environmental Microbiology 77: 8466–77. https://doi.org/10.1128/AEM.05702-11.

10. Yakimov MM, La Cono V, Smedile F, Crisalfi F, Arcadi E, Leonardi M, Decembrini F, Catalfamo M, Bargiela R, Ferrer M, Golyshin PN, Giuliano L (2014) Heterotrophic bicarbonate assimilation is the main process of de novo organic carbon synthesis in hadal zone of the Hellenic Trench, the deepest part of the Mediterranean Sea. Environmental Microbiology Reports 6: 709-722.

11. Baltar F, Lundin D, Palovaara J, Lekunberri I, Reinthaler T, Herndl GJ, Pinhassi J (2016) Prokaryotic responses to ammonium and organic carbon reveal alternative CO2 fixation pathways and importance of alkaline phosphatase in the mesopelagic North Atlantic. Frontiers in Microbiology 7: 1670. https://doi.org/10.3389/fmicb.2016.01670

12. Rogers AD, Frinault BAV, Barnes DKA, Bindoff NL, Downie R, Ducklow HW, et al. (2020). Antarctic Futures: An Assessment of Climate-Driven Changes in Ecosystem Structure, Function, and Service Provisioning in the Southern Ocean. Annual Reviews of Marine Science 12: 7.1-7.34. doi:10.1146/annurev-marine-010419-011028.

13. Turner J, Comiso JC, Marshall GJ, Lachlan-Cope TA, Bracegirdle T, Maksym T, et al. (2009) Non-annular atmospheric circulation change induced by stratospheric ozone depletion and its role in the recent increase of Antarctic sea ice extent. Geophysical Research Letters 36: 1–5. https://doi.org/10.1029/2009GL037524.

14. Hauck J, Völker C, Wolf-Gladrow DA, Laufkötter C, Vogt M, Aumont O et al. (2015). A multi-model study on the Southern Ocean CO2 uptake and the role of the biological carbon pump in the 21st century. Global Biogeochemical Cycles 29, 1451-1470. https://doi.org/10.1002/2015GB005140

15. Strzepek RF, Maldonado MT, Hunter KA, Frew RD, Boyd PW (2011). Adaptive strategies by Southern Ocean phytoplankton to lessen iron limitation: Uptake of organically complexed iron and reduced cellular iron requirements. Limnology and Oceanography 56: 1983–2002. https://doi.org/10.4319/lo.2011.56.6.1983.

16. Boyd PW, Arrigo KR, Strzepek R, Van Dijken GL (2012). Mapping phytoplankton iron utilization: Insights into Southern Ocean supply mechanisms. Journal of Geophysical Research 117, C06009. https://doi.org/10.1029/2011JC007726.

17. Smetacek V, Nicol S (2005) Polar ocean ecosystems in a changing world. Nature 437, 362–368. doi: 10.1038/nature04161

18. Arrigo KR, van Dijken GL, Bushinsky S (2008) Primary production in the Southern Ocean. Journal of Geophysical Research 113:C08004. https://doi.org/10.1029/2007JC004551

19. Smith, WO, Ainley DG, Arrigo KR, Dinniman MS (2014) The oceanography and ecology of the Ross Sea. Annual Review of Marine Science 6, 469-487. doi: 10.1146/annurev-marine-010213-135114

20. Catalano G, Budillon G, La Ferla R, Povero P, Ravaioli M, Saggiomo V, Accornero A, Azzaro M, Carrada GC, Giglio F, Langone L, Mangoni O, Misic C, Modigh M (2009). “The Ross Sea”, in Carbon and Nutrient Fluxes in Continental Margins: A Global Synthesis, eds. L Liu, K-K, Atkinson L, Quinones R, Talaue-McManus (Verlag Berlin Heidelberg: Springer), 303-317.

21. Wefer G, Fischer G (1991) Annual primary production and export flux in the Southern Ocean from sediment trap data. Marine Chemistry 35: 597-613. https://doi.org/10.1016/S0304-4203(09)90045-7

22. Manganelli M, Malfatti F, Samo TJ, Mitchell BG, Wang H, Azam F (2009) Major role of microbes in the carbon fluxes during austral winter in the South Drake Passage. Plos ONE 4: e6941. doi:10.1371/journal.pone.0006941

23. Budillon G, Pacciaroni M, Cozzi S, Rivaro P, Catalano G, Ianni C, Cantoni C (2003) An optimum multiparameter mixing analysis of the shelf waters in the Ross Sea. Antarctic Science 15: 105-118. https://doi.org/10.1017/S095410200300110X

24. Johnson GC (2008) Quantifying Antarctic Bottom Water and North Atlantic Deep Water volumes. Journal of Geophysical Research 113: C05027. https://doi.org/10.1029/2007JC004477

25. Lumpkin R, Speer K (2007) Global ocean meridional overturning. Journal of Physical Oceanography 37: 2550-2562. https://doi.org/10.1175/JPO3130.1

26. Orsi HO, Wiederwhohl CL (2009) A recount of Ross Sea waters. Deep-Sea Research II 56: 778-795. https://doi.org/10.1016/j.dsr2.2008.10.033

27. Rivaro P, Massolo S, Bergamasco A, Castagno P, Budillon G (2010) Chemical evidence of the changes of Antarctic Bottom Water ventilation in the western Ross Sea between 1997 and 2003. Deep-Sea Research I 57: 639-652. https://doi.org/10.1016/j.dsr.2010.03.005

28. Ingrosso G, Giani M, Kralj M, Comici C, Rivaro P, Budillon G, Castagno P, Zoccarato L, Celussi M (2022) Physical and biological controls on anthropogenic CO2 sink of the Ross Sea. Frontiers in Marine Science 9: 954059. doi: 10.3389/fmars.2022.954059

29. Lønborg C, Álvarez-Salgado XA (2012) Recycling versus export of bioavailable dissolved organic matter in the coastal ocean and efficiency of the continental shelf pump. Global Biogeochemical Cycles 26: GB 3018. https://doi.org/10.1029/2012GB004353

30. Azam F, Long RA (2001) Sea snow microcosms. Nature 414: 495-498.

31. Giering SL, Evans C (2022) Overestimation of prokaryotic production by leucine incorporation – and how to avoid it. Limnology and Oceanography 67: 726-738. https://doi.org/10.1002/lno.12032

32. Burd AB, Hansell DA, Steinberg DK, Anderson TR, Arístegui J, Baltar F, Beaupré SR, Buesseler KO, DeHairs F, Jackson GA, Kadko DC, Koppelmann R, Lampitt RS, Nagata T, Reinthaler T, Robinson C, Robison BH, Tamburini C, Tanaka T (2010) Assessing the apparent imbalance between geochemical and biochemical indicators of meso- and bathypelagic biological activity: what the @$#! is wrong with present calculations of carbon budgets? Deep-Sea Research II 57: 1557-1571. https://doi.org/10.1016/j.dsr2.2010.02.022

33. Arístegui J, Gasol JM, Duarte CM, Herndl GJ (2009) Microbial oceanography of the dark ocean's pelagic realm. Limnology and Oceanography 54: 1501-1529. https://doi.org/10.4319/lo.2009.54.5.1501

34. Bayer B, Vojvoda J, Reinthaler T, Reyes C, Pinto M, Herndl GJ (2019) Nitrosopumilus adriaticus sp. nov. and Nitrosopumilus piranensis sp. nov., two ammonia-oxidizing archaea from the Adriatic Sea and members of the class Nitrosphaeria. International Journal of Systematic and Evolutionary Microbiology 69: 1892-1902. https://doi.org/10.1099/ijsem.0.003360

35. Celussi M, Quero GM, Zoccarato L, Franzo A, Corinaldesi C, Rastelli E, Lo Martire M, Galand PE, Ghiglione J-F, Chiggiato J, Coluccelli A, Russo A, Pallavicini A, Fonda Umani S, Del Negro P, Luna GM (2018) Planktonic prokaryote and protist communities in a submarine canyon system in the Ligurian Sea

(NW Mediterranean). Progress in Oceanography 168: 210-221. https://doi.org/10.1016/j.pocean.2018.10.002

36. Vick-Majors TJ, Achberger A, Santibáñez P, Dore JE, Hodson T, Michaud AB, Christner BC, Mikucki J, Skidmore ML, Powell R, Adkins WP, Barbante C, Mitchell A, Scherer R, Priscu JC (2016) Biogeochemistry and microbial diversity in the marine cavity beneath the McMurdo Ice Shelf, Antarctica. Limnology and Oceanography 61: 572-586. https://doi.org/10.1002/lno.10234

37. Manna V, Malfatti F, Banchi E, Cerino F, De Pascale F, Franzo A, Schiavon R, Vezzi A, Del Negro P, Celussi M (2020) Prokaryotic response to phytodetritus-dervied organic material in epi- and mesopelagic Antarctic waters. Frontiers in Microbiology 11, 1242. doi: 10.3389/fmicb.2020.01242

38. Martínez-Pérez C, Greening C, Bay SK, Lappan RJ, Zhao Z, De Corte D, Hulbe C, Ohneiser C, Stevens C, Thomson B, Stepanauskas R, González JM, Logares R, Herndl GJ, Morales SE, Baltar F (2022) Phylogenetically and functionally diverse microorganisms reside under the Ross Ice Shelf. Nature Communications, 13, 117. https://doi.org/10.1038/s41467-021-27769-5

39. Reinthaler T, van Aken H, Herndl GJ (2010) Major contribution of autotrophy to microbial cycling in the deep North Atlantic interior. Deep-Sea Research II 57:1572-1580. https://doi.org/10.1016/j.dsr2.2010.02.023

40. Braun A, Spona-Friedl M, Avramov M, Elsner M, Baltr F, Reinthaler T, Herndl GJ, Griebler C (2021) Reviews and syntheses: heterotrophic fixation of inorganic carbon – significant but invisible flux in environmental carbon cycling. Biogeosciences 18: 3689-3700. https://doi.org/10.5194/bg-18-3689-2021

41. Manna V, Balestra C, Banchi E, Fonti, V, Kralj M, Celussi, M (2025) High contribution of dark dissolved inorganic carbon uptake to microbial carbon cycling in a shallow Mediterranean basin. Ocean Microbiology 1: 2. https://doi.org/10.1186/s44375-025-00002-0.

42. Zoccarato L, Pallavicini A, Cerino F, Fonda Umani S, Celussi M (2016) Water mass dynamics shape Ross Sea protist communities in mesopelagic and bathypelagic layers. Progress in Oceanography 149: 16-26. https://doi.org/10.1016/j.pocean.2016.10.003

43. Mangoni O, Saggiomo V, Bolinesi F, Escalera L, Saggiomo M (2018) A review of past and present summer primary production processes in the Ross Sea in relation to changing ecosystem. Ecological Questions 29: 75-85. https://dx.doi.org/10.12775/EQ.2018.024

44. Parada AE, Needham DM, Fuhrman JA (2016). Every base matters: assessing small subunit rRNA primers for marine microbiomes with mock communities, time series and global field samples. Environmental Microbiology 18: 1403–1414. https://doi.org/10.1111/1462-2920.13023.

45. Klindworth A, Pruesse E, Schweer T, Peplies J, Quast C, Horn M et al (2013) Evaluation of general 16S ribosomal RNA gene PCR primers for classical and next-generation sequencing-based diversity studies. Nucleic Acids Res. 41:e1. https://doi.org/10.1093/nar/gks808

46. Hoshino T, Doi H, Uramoto GI, Wörmer L, Adhikari RR, Xiao N, et al. (2020). Global diversity of microbial communities in marine sediment. Proceedings of the National Academy of Sciences of the USA 117(44): 27587-27597.

47. Könneke M, Schubert DM, Brown PC, Berg IA (2014) Ammonia-oxidizing archaea use the most energy-efficient aerobic pathway for CO2 fixation. Proceedings of the National Academy of Science of the USA 11: 22. https://doi.org/10.1073/pnas.1402028111

48. Srivastava A, De Corte D, Garcia JAL, Swan B, Stepanauskas R, Herndl GJ, Sintes E (2023) Interplay between autotrophic and heterotrophic prokaryotic metabolism in the bathypelagic real revealed by metatranscriptomic analyses. Microbiome 11: 239. https://doi.org/10.1186/s40168-023-01688-7

49. Priest T, von Appen W-J, Oldenburg E, Popa O, Torres-Valdés S, Bienhold C, Metfies K, Boulton W, Mock T, Fuchs BM, Amann R, Boetius A, Wietz M (2023) Atlantic water influx and sea-ice cover drive taxonomic and functional shifts in Arctic marine bacterial communities. The ISME Journal 17: 1612-1625. https://doi.org/10.1038/s41396-023-01461-6

50. Celussi M, Bergamasco A, Cataletto B, Fonda Umani S, Del Negro P (2010) Water masses bacterial community structure and microbial activities in the Ross Sea (Antarctica). Antarctic Science 22: 361-370. https://doi.org/10.1017/S0954102010000192

51. Wilkins D, van Sebille E, Rintoul SR, Lauro FM, Cavicchioli R (2013) Advection shapes Southern Ocean microbial assemblages independent of distance and environmental effect. Nature Communications 4: 2457. https://doi.org/10.1038/ncomms3457

52. Quero GM, Celussi M, Relitti F, Kovačević V, Del Negro P, Luna GM (2020) Inorganic and Organic carbon uptake processes and their connection to microbial diversity in meso- and bathypelagic Arctic waters (Western Fram Strait). Microbial Ecology 79: 823-839. https://doi.org/10.1007/s00248-019-01451-2

53. Agogué H, Lamy D, Neal PR, Sogin ML, Herndl GJ (2011) Water mass-specificity of bacterial communities in the North Atlantic revealed by massive parallel sequencing. Molecular Ecology 20: 258-274. https://doi.org/10.1111/j.1365-294X.2010.04932.x

54. Quero GM, Retelletti Brogi S, Santinelli C, Luna GM (2023) Water mass age and dissolved organic matter properties drive the diversity of pelagic prokaryotes in the Western Mediterranean Sea. Deep-Sea Research I 196: 104022. https://doi.org/10.1016/j.dsr.2023.104022

55. Celussi M, Cataletto B, Fonda Umani S, Del Negro P (2009) Depth profiles of bacterioplankton assemblages and their activities in the Ross Sea. Deep-Sea Research I 56: 2193-2205. https://doi.org/10.1016/j.dsr.2009.09.001

56. Sow SLS, Brown MV, Clarke LJ, Bissett A, van de Kamp J, Trull TW, Raes EJ, Seymour JR, Bramucci AR, Ostrowski M, Boyd PW, Deagle BE, Pardo PC, Sloyan BM, Bodrossy L (2022) Biogeography od Southern Ocean prokaryotes: comparison of the Indian and Pacific sectors. Environmental Microbiology 24: 2449-2466. https://doi.org/10.1111/1462-2920.15906

57. Middelburg JJ (2011) Chemoautotrophy in the ocean. Geophysical Research Letters 38:L24604. https://doi.org/10.1029/2011GL049725

58. Pajares S (2021) Unraveling the distribution patterns of bacterioplankton in a mesoscale cyclonic eddy confined to an oxygen-depleted basin. Aquatic Microbial Ecology 87: 151-166. https://doi.org/10.3354/ame01975

59. Celussi M, Manna V, Banchi E, Fonti V, Bazzaro M, Flander-Putrle V, Klun K, Kralj M, Orel N, Tinta T (2024) Annual recurrence of prokaryotic climax communities in shallow waters of the North Mediterranean. Environmental Microbiology 26: e16595. https://doi.org/10.1111/1462-2920.16595

60. Baltar F, Martínez-Pérez C, Amano C; Vial M, Robaina-Estévez S, Reinthaler T, Herndl GJ, Zhao Z, Logares R, Morales SE, González JM (2023) A ubiquitous gammaproteobacterial clade dominates expression of sulfur oxidation genes across the mesopelagic ocean. Nature Microbiology 8: 1137-1148. https://doi.org/10.1038/s41564-023-01374-2

61. Boeuf D, Eppley JM, Mende DR, Malmstrom RR, Woyke T, DeLong EF (2021) Metapangenomics reveals depth-dependent shifts in metabolic potential for the ubiquitous marine bacterial SAR324 lineage. Microbiome 9: 172. https://doi.org/10.1186/s40168-021-01119-5

62. Callbeck CM, Canfield DE, Kuypers MMM, Yimaz P, Lavik G, Thamdrup B, Schubert CJ, Bristow LA (2021) Sulfur cycling in oceanic oxygen minimum zones. Limnology and Oceanography 66: 2360-2392. https://doi.org/10.1002/lno.11759

63. He Y, Baltar F, Wang Y (2025) Seasonal variability in community structure and metabolism of active deep-sea microorganisms. The ISME Journal 16: wraf214. https://doi.org/10.1093/ismejo/wraf214

64. Bergamasco A, Defendi V, Del Negro P, Fonda Umani S (2003) Effects of the physical properties of water masses on microbial activity during an Ice Shelf Water overflow in the central Ross Sea. Antarctic Science 15: 405-411. https://doi.org/10.1017/S0954102003001421

65. Hansen HP, Koroleff F (1999) Determination of nutrients. In Methods of Seawater Analysis (eds Grasshoff K, Kremling K, Ehrhardt M). https://doi.org/10.1002/9783527613984.ch10 (1999).

66. Kirchman DL, K'nees E, Hodson R (1985) Leucine incorporation and its potential as a measure of protein synthesis by bacteria in natural aquatic systems. Applied and Environmental Microbiology 49: 599–607.

67. Ducklow HW, Dickson M-L, Kirchman DL, Steward G, Orchardo J, Marra J, Azam F (2000) Constrainng bacterial production, conversion efficiency and respiration in the Ross Sea, Antarctica, January-February, 1997. Deep-Sea Research II 47: 3227-3247. https://doi.org/10.1016/S0967-0645(00)00066-7

68. Kirchman DL, Meon B, Ducklow HW, Carlson CA, Hansell Steward GF (2001) Glucose fluxes and concenrations of dissolved combined neutral sugars (polysaccharides) in the Ross Sea and Polar Fron Zone, Antarctica. Deep-Sea Research II 48:4179-4197. https://doi.org/10.1016/S0967-0645(01)00085-6

69. Smith DC, Azam F (1992) A simple, economical method for measuring bacterial protein synthesis rates in sea water using 3H-leucine. Marine Microbial Food Webs 6: 107–114.

70. Kirchman DL, Ducklow HW (1993) Estimating conversion factors for thymidine and leucine methods for measuring bacterial production. In Handbook of Methods in Aquatic Microbial Ecology. Kemp P, Sherr BF, Sherr EB, Cole JJ (eds.). Boca Raton, FL, USA: Lewis, pp. 513–517.

71. Packard TT, and Williams PJLeB (1981) Rates of respiratory oxygen consumption and electron transport in surface seawater from the Northwest Atlantic. Oceanologica Acta 4: 531–358.

72. Reinthaler T, van Aken H, Veth C, Arıstegui J, Robinson C, Williams PJ, et al. (2006) Prokaryotic respiration and production in the meso- and bathypelagic realm of the eastern and western North Atlantic basin. Limnology and Oceanography 51: 1262–1273. https://doi.org/10.4319/lo.2006.51.3.1262

73. Arıstegui J, Duarte CM, Gasol JM, Alonso-Saez L (2005) Active mesopelagic prokaryotes support high respiration in the subtropical northeast Atlantic Ocean. Geophysical Research Letters 32: L03608. https://doi.org/10.1029/2004GL021863

74. Steeman Nielsen E (1952) The use of radioactive 14C for measuring organic production in the sea. Journal du Conseil International pour l'Exploration de la Mer 18: 117-140.

75. Fadeev E, Cardozo-Mino MG, Rapp JZ, Bienhold C, Salter I, Salman-Carvalho V, et al. (2021). Comparison of two 16S rRNA primers (V3–V4 and V4–V5) for studies of arctic microbial communities. Frontiers in Microbiology 12: 637526. https://doi.org/10.3389/fmicb.2021.637526

76. Martin M (2011) Cutadapt removes adapter sequences from high-throughput sequencing reads. EMBnet J. 17:10–2.

77. RStudio-Team, (2020). RStudio: Integrated Development for R. Boston, MA: RStudio.

78. Callahan BJ, McMurdie PJ, Rosen MJ, Han AW, Johnson AJA, Holmes SP (2016) DADA2: high-resolution sample inference from Illumina amplicon data. Nature Methods 13: 581–583. https://doi.org/10.1038/nmeth.3869

79. Quast C, Pruesse E, Yilmaz P, Gerken J, Schweer T, Yarza P, Peplies J, Glöckner FO (2013) The SILVA ribosomal RNA gene database project: improved data processing and web-based tools. Nucleic Acids Research 41:590–596. https://doi.org/10.1093/nar/gks1219

80. Wickham H. Programming with ggplot2. Inggplot2 2016 (pp. 241-253). Springer, Cham.

81. Oksanen J, Simpson G, Blanchet F, Kindt R, Legendre P, Minchin P, O'Hara R, Solymos P, Stevens M, Szoecs E, Wagner H, Barbour M, Bedward M, Bolker B, Borcard D, Borman T, Carvalho G, Chirico M, De Caceres M, Durand S, Evangelista H, FitzJohn R, Friendly M, Furneaux B, Hannigan G, Hill M, Lahti L, Martino C, McGlinn D, Ouellette M, Ribeiro Cunha E, Smith T, Stier A, Ter Braak C, Weedon J (2025). *vegan: Community Ecology Package*. R package version 2.8-0, https://vegandevs.github.io/vegan/.

82. Kutner DS, Bowman JS, Saldanha-Correa FMP, Chuqui MG, Tura PM, Moreira DL, Brandini FP, Signori CN (2023) Inorganic carbon assimilation by planktonic community in Santos Basin, Southwest Atlantic Ocean. Ocean and Coastal Research v71: e23006. http://doi.org/10.1590/2675-2824071.22085dsk

83. Baltar, F., Arístegui, J., Sintes, E., Gasol J. M., Reinthaler, T. & Herndl, G. J. Significance of non-sinking particulate organic carbon and dark CO2 fixationto heterotrophic carbon demand in the mesopelagic northeast Atlantic. *Geophys. Res. Lett.* **37**, L09602 (2010). https://doi.org/10.1029/2010GL043105

84. Saxena H, Sahoo D, Nizirahmed S, Rai DK, Khan MA, Sharma N, Kumar S, Singh A (2022) Contribution of carbon fixation toward carbon sink in the ocean twilight zone. Geophysical Research Letters 49, e2022GL099044. https://doi.org/10.1029/2022GL099044

85. Bayer B, Kitzinger K, Paul NL, Albers JB, Saito MA, Wagner M, Carlson CA, Santoro AE (2025) Minor contribution of ammonia oxidizers to inorganic carbon fixation in the ocean. Nature Geoscience 18: 1144–1151. https://doi.org/10.1038/s41561-025-01798-x

86. Yakimov MM, La Cono V, Smedile F et al. (2011) Contribution to crenarchaeal autotrophic ammonia oxidizers to the dark primary production in Tyrrhenian deep waters. The ISME Journal 5: 945-961. https://doi.org/10.1038/ismej.2010.197

87. Schlitzer R (2018) Ocean Data View. https://odv.awi.de

Acknowledgements

The authors are grateful to I. Biagiotti, G. Canduci, G. De Carolis (CNR), D. Cotterle, R. Geletti (OGS), E. Colizza (UNITS), the crew of the R/V Italica, and the team from ENEA for their help during sampling. We are grateful to C. Comici, M. Kralj, F. Relitti (OGS) and L. Zoccarato (UNITS) for chemical data and microscopy cell counts.

Funding statement

This study was supported by the project DEEPROSSS (DEEP ROSS Sea ecosystem functioning: new insights on the role of ventilation on microbial metabolism and diversity) in the framework of the Italian Program for Research in Antarctica (project PNRA 2013/AN1.01) with funds from the Italian Ministry of Education, University and Research (MIUR).

Author Contribution

M.C. conceived the study. M.C. and G.M.L. contributed to the sampling and experimental design. M.C., G.M.Q., E.B., M.B., performed laboratory analyses. G.M.Q., E.B., M.B. conducted metabarcoding and bioinformatic analyses. M.C., V.M., G.B., P.C., A.P.R., G.M.L. contributed to data interpretation. M.C., V.M., M.B., data visualization. M.C. drafted the first version of the manuscript. All authors contributed to the manuscript preparation in its final version.

Competing interest

The authors declare no competing interest.

Figure captions

Figure 1: Map of the sampling stations in the Ross Sea (Southern Ocean). Station names beginning with 'A' were sampled in 2014; those identified by numbers only were sampled in 2016. In the lower panel the main geographical dynamics of the three water masses are reported: High Salinity Shelf Water – HSSW in green; Circumpolar Deep Water – CDW in white; Antarctic Bottom Water – AABW- in red.

Outside of the shelf break AABW spreads underneath CDW. The water mass circulation diagram is a simplification of the original version by Budillon et al. (2003)[23]. The maps were created with the ODV software[87].

Figure 2: Organic matter concentration and features of the three water masses. Box-whiskers plots [box = interquartile range with median; whiskers = range without outliers] of Dissolved Organic Carbon (DOC) concentration, of the ratio between organic C and N in the dissolved phase, of the Particulate Organic Carbon (POC) concentration and of the ratio between organic C and N in the particulate phase in High Salinity Shelf Water (HSSW, left boxes), Antarctic Bottom Water (AABW, central boxes) and Circumpolar Deep Water (CDW, right boxes). Letters above boxes refer to results of the Kruskal-Wallis ANOVA, followed by the post hoc Dunn's test ($p < 0.05$). Different letters indicate significant differences among water masses.

Figure 3: Microbial activities in the three water masses. Box-whiskers plots [box = interquartile range with median; whiskers = range without outliers] of Dissolved Inorganic Carbon (DIC) fixation rates, Respiration rates measured by the ETS method using the 0.68 conversion factor (CF), Heterotrophic Carbon Production rates and Prokaryotic Growth Efficiency, in High Salinity Shelf Water (HSSW, left boxes), Antarctic Bottom Water (AABW, central boxes) and Circumpolar Deep Water (CDW, right boxes). Letters above boxes refer to results of the Kruskal-Wallis ANOVA followed by the post hoc Dunn's test ($p < 0.05$). Different letters indicate significant differences among water masses.

Figure 4: Non-metric multidimensional scaling (nMDS) performed on the 16S rRNA bacterial gene dataset using a Jaccard dissimilarity matrix and average linkage approach. Samples collected in High Salinity Shelf Water (HSSW) are reported in green, those collected in Antarctic Bottom Waters (AABW) are reported in red and those collected in Circumpolar Deep Water (CDW) are reported in white. Convex hulls group together samples from specific water mass and are color-coded accordingly.

Figure 5: Bar plot of the relative abundance of putative chemoautotrophic bacterial taxa. Relative abundances are reported at the highest possible taxonomic resolution assigned with the Silva database. Labels indicate station_depth. Significant differences between the relative abundance of taxa in High Salinity Shelf Water (HSSW) and Circumpolar Deep Water (CDW) are highlighted in Supplementary Table 3.

Table 1: DIC fixation rates measured in the major ocean basins at depths greater than 200 m

Ocean	Region	DIC fixation rates	Reference
		nmol C L^{-1} d^{-1}	
Arctic	Eastern Fram Strait	0.08-24.04	52
Atlantic	Central-North Atlantic	0.19-5.36	39
	Santos Basin	4-2200	82

	Subtropical NE Atlantic	12 ± 5	83
Indian	Arabian Sea	0.5-6	84
Pacific	Eastern tropical/subtropical Pacific	0.3-1.9	85
Mediterranean Sea	Tyrrhenian Sea	4.16-19.16	86
	whole basin	0.57-240.42	3
Southern	Southern Drake Passage	0.01-3.33	22
	Ross Sea	0.20-0.71[a]	37
	Ross Sea	0.03-3.12	this study
	Ross Sea, McMurdo Ice Shelf cavity	6.0 ± 1.0	36

[a] Measured on the 0.2-1 µm fraction

Editorial summary:
Microbial carbon fixation in deep waters below the illuminated water column accounts for ~5% of the annual dissolved inorganic carbon sink in the Ross Sea, according to incubation experiments replicating Antarctic waters between 200 m and 2000 m depth

Peer review information:

Communications Earth and Environment thanks Guang-Chao Zhuang and the other, anonymous, reviewer(s) for their contribution to the peer review of this work. Primary Handling Editors: José Luis Iriarte Machuca, Joe Aslin and Alireza Bahadori. A peer review file is available.

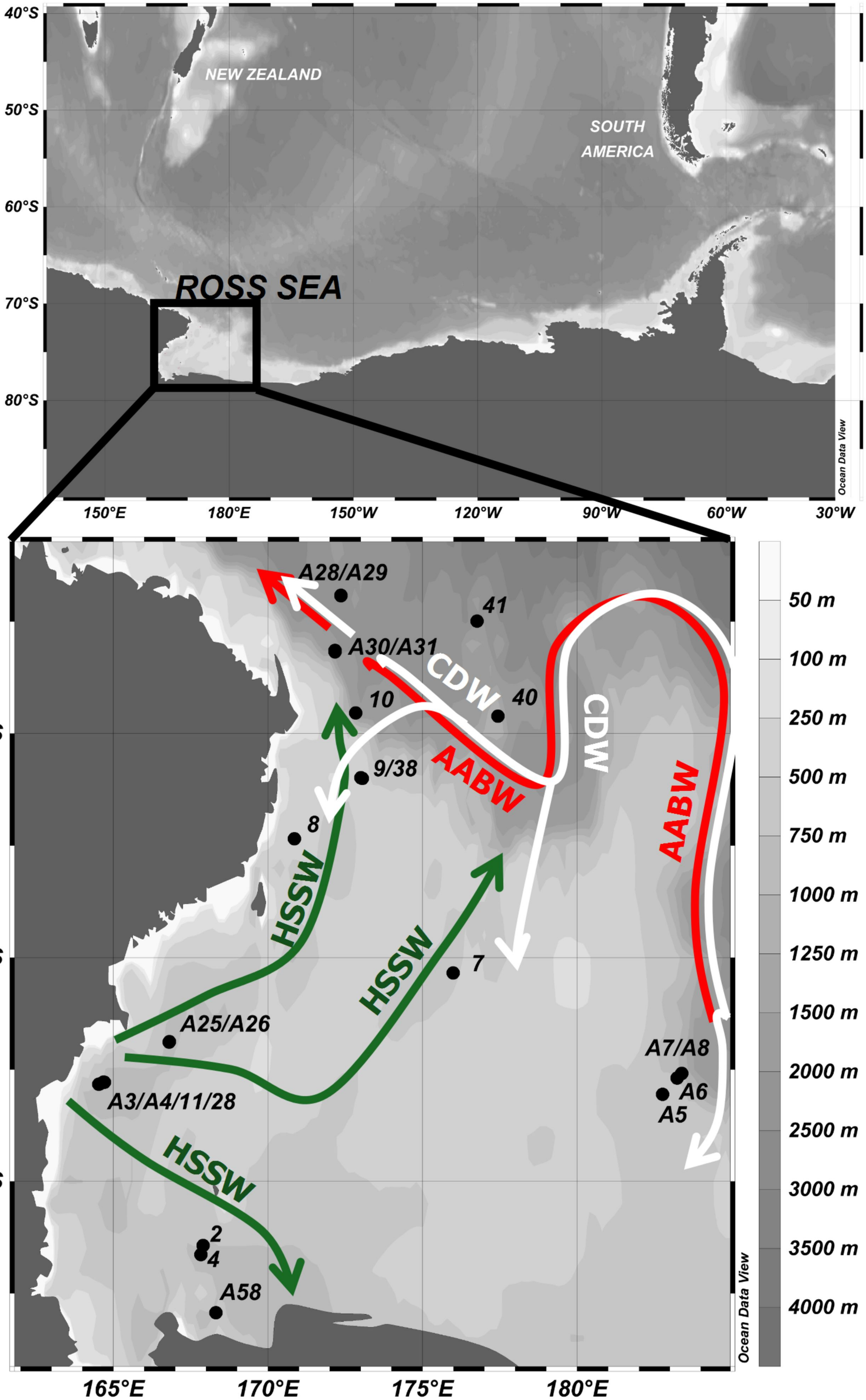
40°S
50°S
60°S
70°S
80°S
NEW ZEALAND
SOUTH AMERICA
ROSS SEA
150°E
180°E
150°W
120°W
90°W
60°W
30°W
Ocean Data View
A28/A29
41
A30/A31
CDW
40
10
9/38
AABW
8
HSSW
HSSW
7
HSSW
A25/A26
A3/A4/11/28
A7/A8
A6
A5
2
4
A58
72°S
74°S
76°S
165°E
170°E
175°E
180°E
50 m
100 m
250 m
500 m
750 m
1000 m
1250 m
1500 m
2000 m
2500 m
3000 m
3500 m
4000 m
Ocean Data View

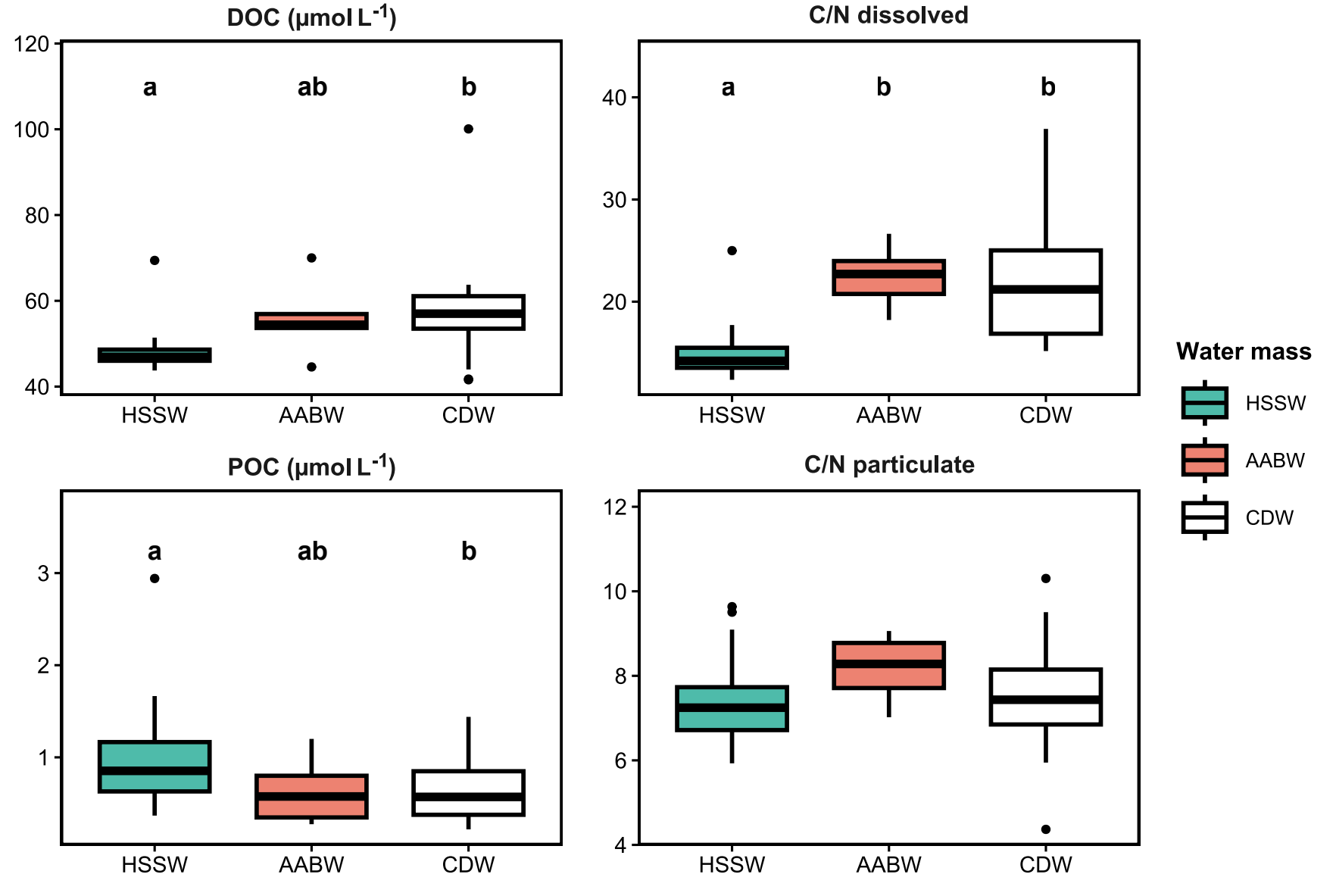
DOC (µmol L-1)
120
100
80
60
40
a
ab
b
HSSW
AABW
CDW
C/N dissolved
40
30
20
a
b
b
HSSW
AABW
CDW
POC (µmol L-1)
3
2
1
a
ab
b
HSSW
AABW
CDW
C/N particulate
12
10
8
6
4
HSSW
AABW
CDW
Water mass
HSSW
AABW
CDW

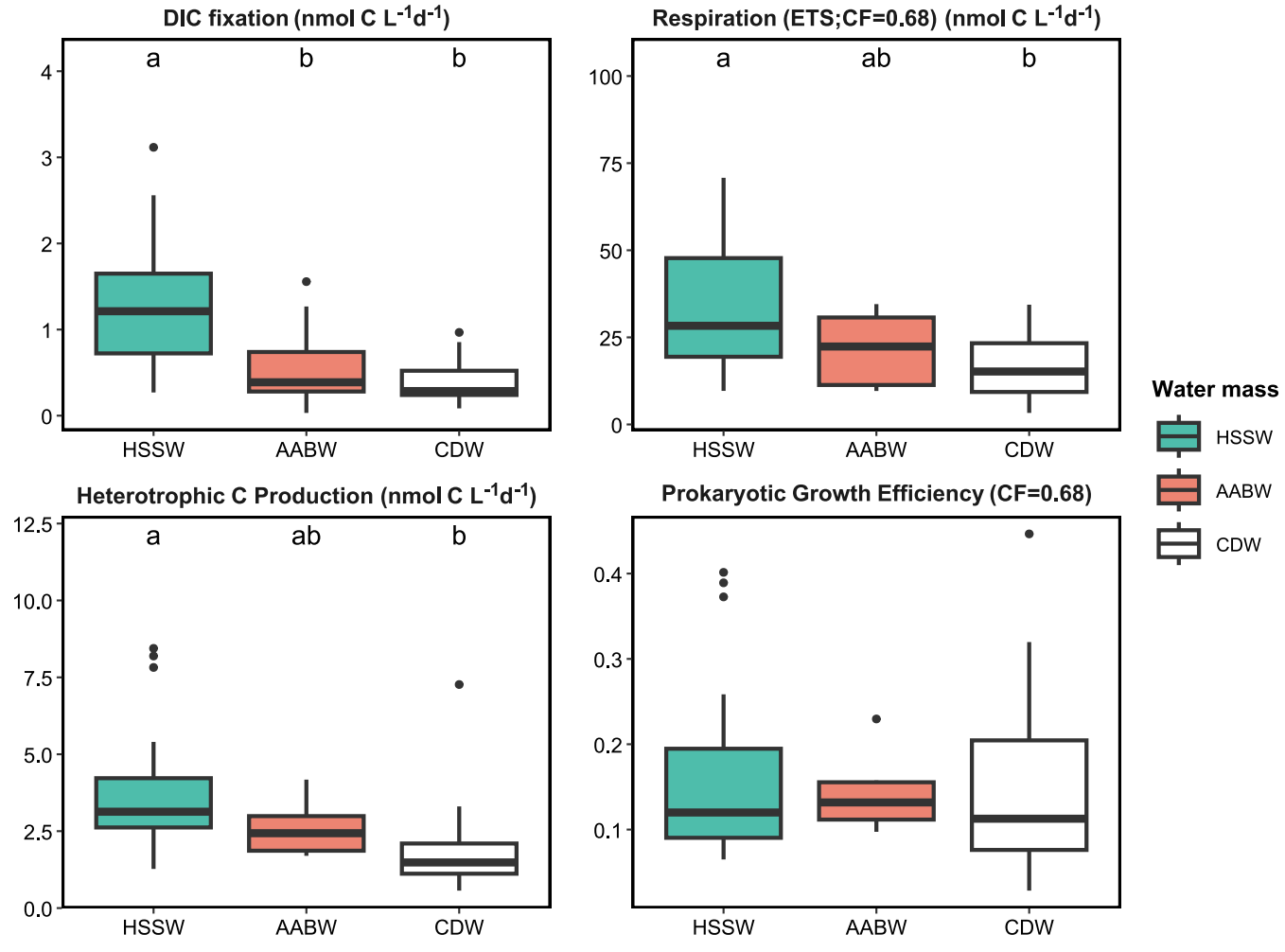
DIC fixation (nmol C L-1d-1)
a
b
b
4
3
2
1
0
HSSW
AABW
CDW
Respiration (ETS;CF=0.68) (nmol C L-1d-1)
a
ab
b
100
75
50
25
0
HSSW
AABW
CDW
Heterotrophic C Production (nmol C L-1d-1)
a
ab
b
12.5
10.0
7.5
5.0
2.5
0.0
HSSW
AABW
CDW
Prokaryotic Growth Efficiency (CF=0.68)
0.4
0.3
0.2
0.1
HSSW
AABW
CDW
Water mass
HSSW
AABW
CDW

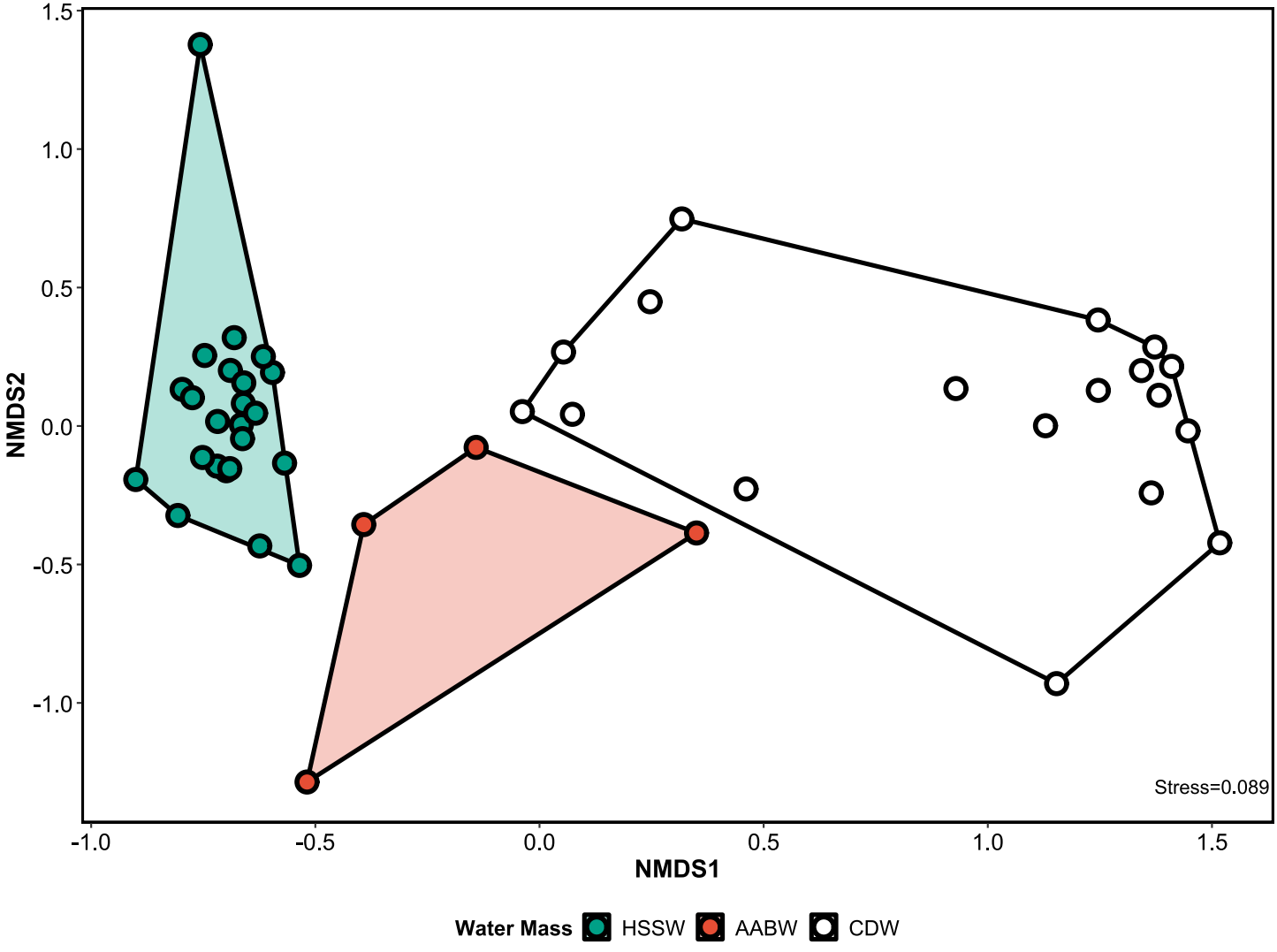
1.5
1.0
0.5
0.0
-0.5
-1.0
NMDS2
-1.0
-0.5
0.0
0.5
1.0
1.5
NMDS1
Stress=0.089
Water Mass
HSSW
AABW
CDW

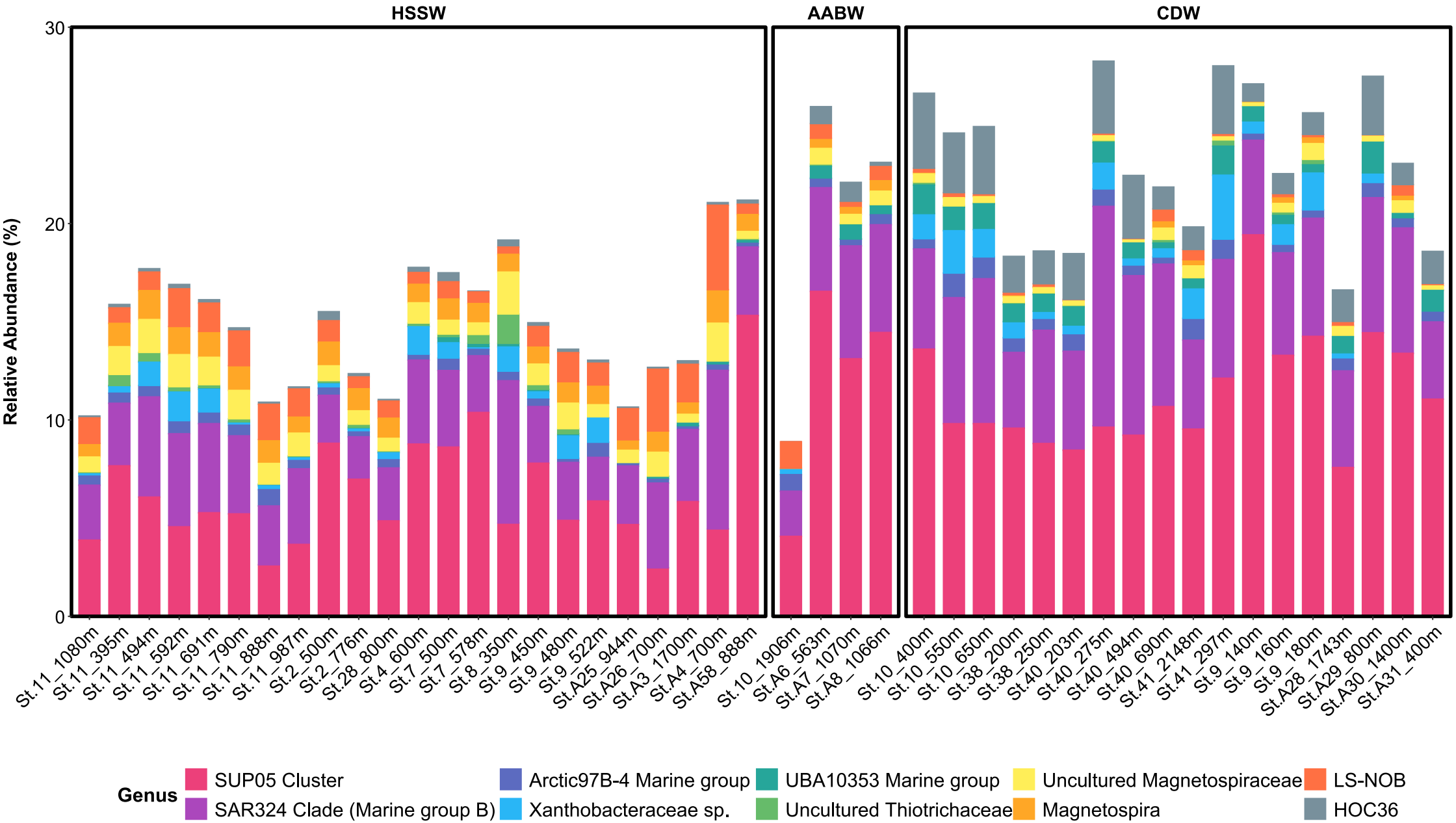
HSSW
AABW
CDW
Relative Abundance (%)
30
20
10
0
St.11_1080m
St.11_395m
St.11_494m
St.11_592m
St.11_691m
St.11_790m
St.11_888m
St.11_987m
St.2_500m
St.2_776m
St.28_800m
St.4_600m
St.7_500m
St.7_578m
St.8_350m
St.9_450m
St.9_480m
St.9_522m
St.A25_944m
St.A26_700m
St.A3_1700m
St.A4_700m
St.A58_888m
St.10_1906m
St.A6_563m
St.A7_1070m
St.A8_1066m
St.10_400m
St.10_550m
St.10_650m
St.38_200m
St.38_250m
St.40_203m
St.40_275m
St.40_494m
St.40_690m
St.41_2148m
St.41_297m
St.9_140m
St.9_160m
St.9_180m
St.A28_1743m
St.A29_800m
St.A30_1400m
St.A31_400m
Genus
SUP05 Cluster
SAR324 Clade (Marine group B)
Arctic97B-4 Marine group
Xanthobacteraceae sp.
UBA10353 Marine group
Uncultured Thiotrichaceae
Uncultured Magnetospiraceae
Magnetospira
LS-NOB
HOC36